Energetics of CO 2 Adsorption on Mg–Al Layered Double Hydroxides and Related Mixed Metal Oxides

ARTICLE *in* THE JOURNAL OF PHYSICAL CHEMISTRY C · NOVEMBER 2014

Impact Factor: 4.77 · DOI: 10.1021/jp508678k

2 AUTHORS, INCLUDING:

Radha Shivaramaiah
University of California, Davis
14 PUBLICATIONS **50** CITATIONS

THE JOURNAL OF PHYSICAL CHEMISTRY C

Article

pubs.acs.org/JPCC

Energetics of CO_2 Adsorption on Mg−Al Layered Double Hydroxides and Related Mixed Metal Oxides

S. Radha and A. Navrotsky*

Peter A. Rock Thermochemistry Laboratory and NEAT ORU, University of California Davis, Davis, California 95616, United States

Supporting Information

ABSTRACT: Energetics of CO_2 uptake by layered double hydroxides (LDH) of Mg and Al and their corresponding mixed metal oxides (MMO) of two different compositions (Mg/Al = 2:1 and 3:1) were investigated by gas adsorption calorimetry. The initial adsorption enthalpies for all the LDH and MMO are similar and in the range −90 to −120 kJ/mol, indicating strong chemisorption of CO_2. However, the differential adsorption enthalpy varies substantially with increasing coverage for different samples. LDH prepared by coprecipitation (both Mg/Al = 2 and 3) and their corresponding MMO exhibit similar CO_2 uptake, which are in the working sorption capacity range (0.6−1 mmol/g), but the one prepared by urea hydrolysis shows poor sorption capacity (0.02−0.35 mmol/g). An integral enthalpy of adsorption of −54 kJ/mol was observed for [Mg−Al−CO_3] LDH prepared by urea hydrolysis and −59 kJ/mol and −57 kJ/mol for the ones prepared by coprecipitation with composition 3:1 and 2:1, respectively. Attenuated total reflectance spectroscopy measurements of samples after CO_2 uptake aid in identifying the mode of binding of adsorbed carbonate, which gives information about strength of basic sites. The presence of monodentate carbonate in all samples suggests that strong basic sites are available in LDH and MMO, in agreement with the large exothermic initial adsorption enthalpies observed, indicating strong chemisorption.

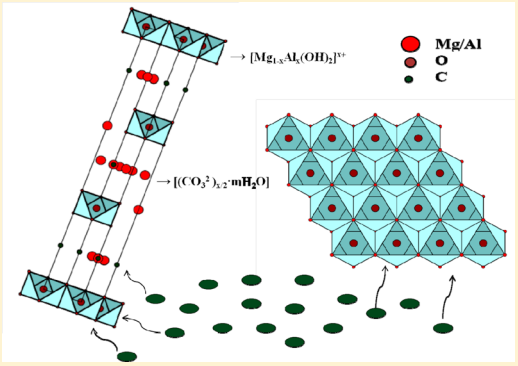

INTRODUCTION

Sequestration of anthropogenic carbon dioxide is one of today's greatest challenges. Several approaches have been adopted to address this concern, including physical, biological, and chemical routes depending on the source of CO_2 generation.[1] Among several chemical strategies, sorption of CO_2 released by fossil fuel combustion using capturing agents/sorbents are an attractive method for CO_2 removal.[2] Stability, scalability, affinity, selectivity, and energy involved during the sorption are the main criteria for an effective CO_2 sorbent. Layered double hydroxides (LDH) are promising for CO_2 capture.[3−5] They are an important class of functional inorganic layered materials which are already used for various applications including flame retardants, drug delivery, anion sorbents, and catalysts.[6−9] LDH are composed of a stacking of positively charged brucite-like layers, having the composition $[M^{II}_{1-x}M'_x{}^{III}(OH)_2]^{x+}$ (M = Mg, Ca, Zn, Co, Ni, Cu, ...; M′ = Al, Cr, Fe, ...) with anions intercalated in the interlayer for charge compensation.[10] Various anions occupy the interlayer gallery ranging from monatomic halides to long chain surfactant ions.[11] LDH have an unusual affinity toward carbonate ions owing to their ability to hydrogen bond with the metal hydroxide layers.[12] Because of their compositional flexibility and structural complexity, they possess energetically different basic sites. LDH also act as a single source precursor for mixed metal oxides, MMO (sometimes also called layered double oxides), which are obtained by thermal decomposition at 400−600 °C.[13] A schematic of structures of LDH and MMO is shown in Figure 1. The MMO have very high surface area with several basic sites and exhibit high catalytic activity.[14] Their basicity can be tuned by the choice of cations in the layer and the composition of the precursor LDH. The MMO pick up CO_2 from ambient air in the presence of moisture and reconstruct back to LDH phases, which is referred to as "memory effect".[15]

$$\text{LDH} \xrightarrow{400\,^\circ\text{C}} \text{MMO}$$
$$\text{MMO} \xrightarrow{CO_2+\text{moisture}} \text{LDH}$$

These properties make LDH and MMO attractive candidates for CO_2 uptake.[16−18] They exhibit high working sorption capacity (0.45−1.0 mol/kg) both at room temperature and at 400−450 °C.[19,20] One of the direct applications foreseen is in the sorption-enhanced water gas shift reaction (SEWGS) at 200−400 °C to maximize H_2 production.[21,22] In this context, there have been several comprehensive studies on the effect of divalent cations, trivalent cations, M^{2+}/M^{3+} ratio and intercalated anions on CO_2 uptake of LDH.[4,23] Wang et al.[24] and Hutson et al.[25] conclude that the Mg−Al carbonate system has highest CO_2 capture capacity. The Mg−O species is

Received: August 27, 2014
Revised: November 19, 2014
Published: November 20, 2014

   dx.doi.org/10.1021/jp508678k | J. Phys. Chem. C 2014, 118, 29836−29844

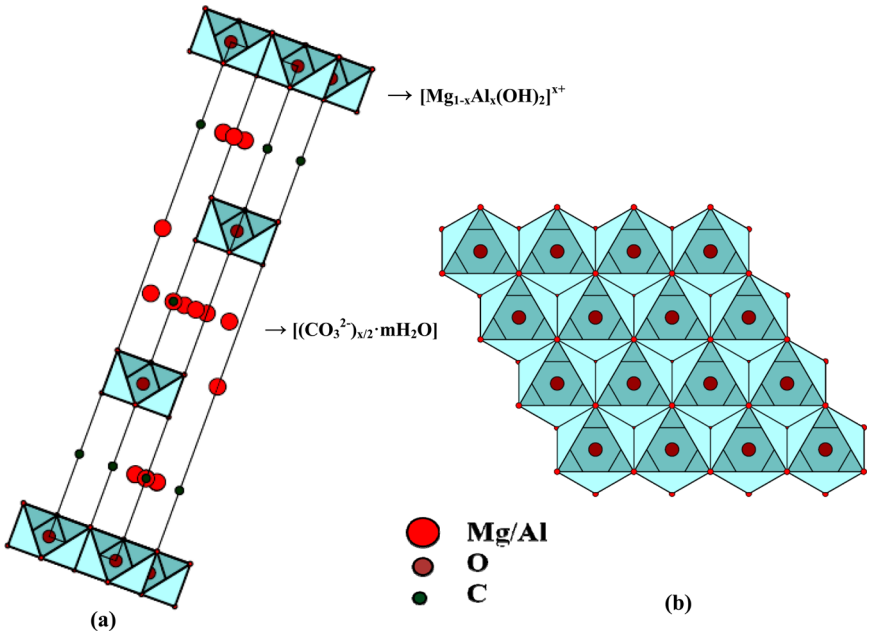

Figure 1. Schematic representation of structures of (a) [Mg−Al−CO_3] layered double hydroxide showing metal hydroxide layers with carbonate and water in the interlayer; (b) its corresponding mixed metal oxide. Shaded blue polyhedra show metal coordination.

proposed to be the active site for CO_2 adsorption.[26] Other factors influencing adsorption capacity include temperature, presence of water and alkali, preparation method, adsorption conditions, reversibility, and regeneration.[27,28]

The CO_2 uptake of LDH is also significant from a geochemical perspective. A recent report on "dynamic breathing of CO_2 by LDH" uses ^{13}C labeling to show the dynamic exchange of intercalated carbonate with carbonate ions derived from atmospheric CO_2 at ambient conditions.[29] As LDH exist in nature these results imply that they actively participate in the carbon cycle involving exchange between the lithosphere and atmosphere. This observation also implies that, unlike suggested in earlier reports,[26] pristine LDH themselves can be used for catalytic conversion of CO_2. Also since LDH can exist as minerals at shallow depths (under appropriate pH and other conditions) in the Earth's critical zone and crust, it is possible that they could participate in the mineralization of CO_2 during geological sequestration.

It is thus very interesting and environmentally relevant to examine the energetics of CO_2 adsorption on LDH and MMO. The energetics of CO_2 sorption can be evaluated by measuring heat of adsorption of CO_2 using calorimetric techniques.[30] CO_2 adsorption on LDH and MMO is both physical and chemical in origin and the enthalpy of CO_2 adsorption obtained by direct calorimetric measurements would be useful to evaluate the strengths of CO_2 binding. Here we report CO_2 sorption energetics of Mg−Al LDH of two different compositions (Mg/Al = 2:1, 3:1) prepared by coprecipitation and by urea hydrolysis and their corresponding MMO.

EXPERIMENTAL METHODS

Synthesis. LDH of different compositions were synthesized by coprecipitation at constant high pH (Riechle method).[31] In a typical synthesis, a $Mg(NO_3)_2$ and $Al(NO_3)_3$ solution of required composition was slowly added to a solution containing 50 mL of NaOH (2 M) and Na_2CO_3 (three times the stoichiometric requirement) under constant stirring. This method ensured a constant high pH during precipitation and aging. The resulting slurry was aged at 70 °C for 18 h. The precipitate was separated by centrifugation and washed with distilled water to remove excess Na_2CO_3 and dried at 60 °C. The synthesized [Mg−Al−CO_3] LDHs are labeled as MA_21 and MA_31 corresponding to 2:1 and 3:1 ratios of Mg/Al, respectively. A highly crystalline LDH sample was synthesized by a urea hydrolysis method,[32] wherein 40 mL of mixed metal nitrate solution (total concentration, 0.5 M) containing ($[M^{II}]/[M^{III}]$) = 2 was mixed with urea ([urea]/[total metal] = 3.5) and hydrothermally treated at 90 °C for 24 h in a Teflon liner sealed in a stainless steel autoclave. The resulting solid was washed with water and dried at 60 °C. This sample is labeled as MA_UH. Mixed metal oxides of all the LDH were synthesized by heating the sample at 400 °C under vacuum for 5 h. All the MMO were stored in airtight vials for their characterization by pwder X-ray diffraction (PXRD) and attenuated total internal reflectance Fourier transform infrared (ATR-FTIR) spectroscopy. For the gas adsorption analysis MMO were prepared in situ where the LDH were heated at 400 °C under vacuum for 5 h using a Setaram Sensys, Calvet microcalorimeter, which was also used for measuring heat effects during gas adsorption.

Characterization. All samples were characterized by PXRD using a Bruker AXS model D8 Advance diffractometer with Cu Ka radiation, Kα = 1.5418 Å, to determine the phases present. PXRD patterns were recorded for the as-prepared samples, samples degassed at 100 and 400 °C, and samples after CO_2 adsorption experiments. In the case of degassed/heat-treated samples and samples after CO_2 adsorption, samples were mounted on an air sensitive sample holder to avoid the effect of moisture and CO_2 in the atmosphere. The specific surface area was measured by the Brunauer−Emmett−Teller (BET) method using a Micromeritics Gemini VII surface area analyzer. The samples were degassed at 100 and 400 °C for 5 h before the measurements to obtain the surface area of pristine LDH and MMO. Measurements were performed soon after degassing to avoid adsorption of water or CO_2 from air. Thermogravimetric analysis (TGA) was performed to determine the water content in the samples using a Netzsch

dx.doi.org/10.1021/jp508678k | J. Phys. Chem. C 2014, 118, 29836−29844

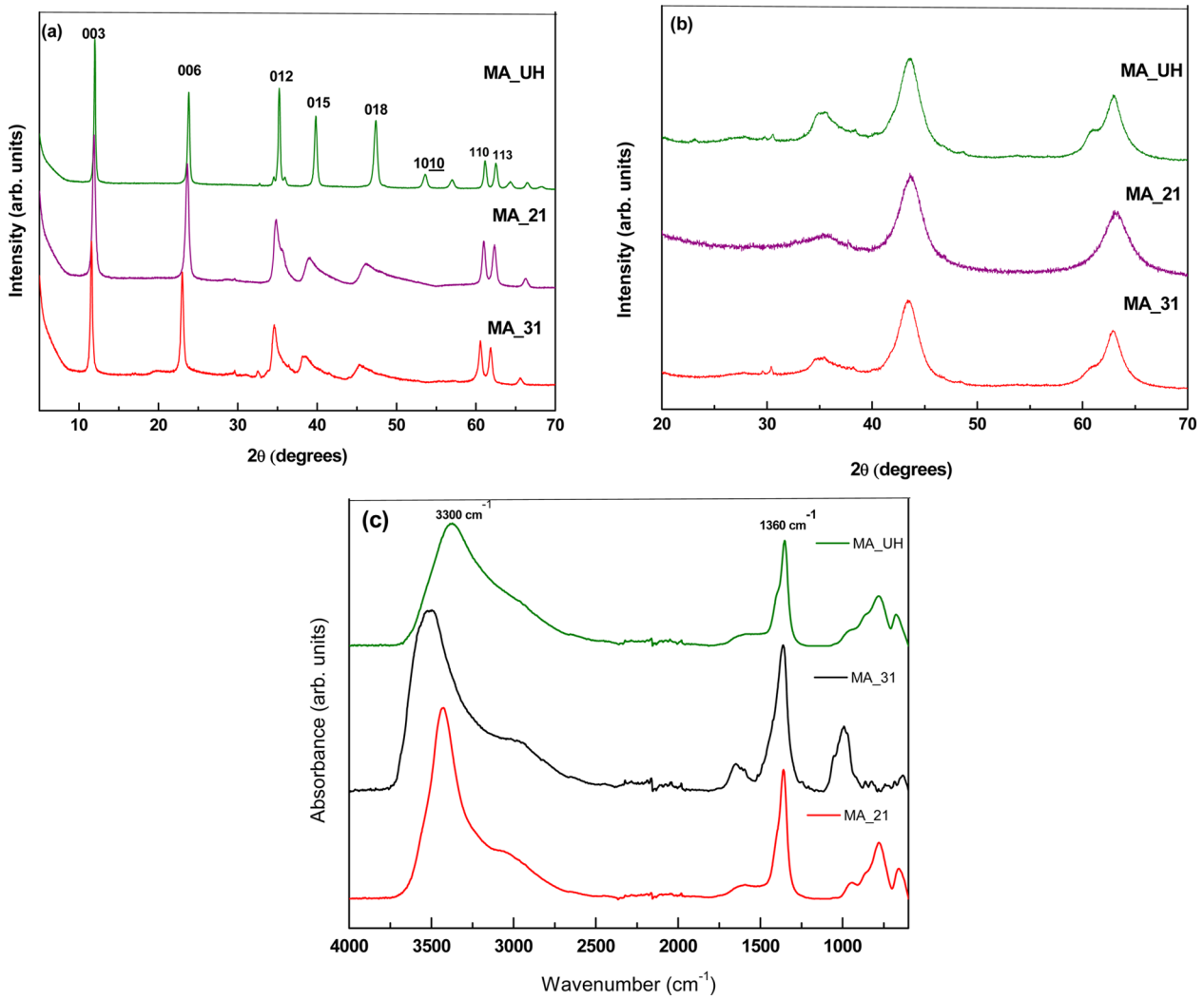

Figure 2. (a) PXRD patterns of MA_31, MA_21, and MA_UH LDH and (b) their corresponding MMO. (c) ATR-FTIR spectra of all the three pristine LDH.

449 thermal analysis system in a dynamic Ar atmosphere (25−800 °C, 5 °C/min, Pt crucible). The data were analyzed using Netzsch Proteus software. The Mg and Al content in the samples were measured by electron microprobe analysis using a Cameca SX 100 instrument operated at 15 kV with 10 mA probe current. Samples were pelletized, sintered, mounted on a probe holder, and polished with diamond paste. ATR-FTIR of all the samples was recorded using a Bruker model Alpha-P IR spectrometer (diamond ATR cell, angle of incidence = 45°, depth of penetration = 1.66 μm, multiple reflection, 4 cm^{-1} resolution, 400−4000 cm^{-1}). ATR-FTIR measurements were made on the samples before and after CO_2 adsorption experiments to examine any changes in carbonate stretching frequencies. The degassed/heat treated samples and the samples after CO_2 uptake were stored in airtight vials in a glovebox before measurements to avoid adsorption of atmospheric H_2O and CO_2. A background scan was performed before recording ATR-FTIR of each sample in order to subtract the contribution from ambient atmosphere around the diamond crystal of ATR. So we consider that there is negligible effect of atmospheric H_2O/CO_2 on the observed spectra. The broad bands observed in some cases were decomposed into Gaussian components using Peakfit version 4.12 software (Peakfit SeaSolve Software). Least squares fitting was performed using the spectroscopic data with no baseline subtraction. Automated fitting was chosen to generate the component bands, and fitting of the observed spectrum was performed to have the goodness of fit parameter ∼1.

CO_2 Adsorption Calorimetry. CO_2 adsorption calorimetric measurements were performed at 25 °C using 100−150 mg samples. The calorimetric system used for the studies is unique and includes a commercial gas adsorption analyzer (Micromeritics ASAP 2020) coupled to a Calvet-type microcalorimeter (Setaram Sensys), as described previously.[29,33] Prior to CO_2 adsorption measurements, each sample was degassed at 100 and 400 °C in different sets of experiments in order to study uptake properties on pristine LDH and MMO. Degassing at 100 °C removes adsorbed water, keeping the layered double hydroxide structure intact, while degassing at 400 °C leads to breakdown of the hydroxide framework leading to amorphous MMO. The gas adsorption calorimetry experiments were then started at 25 °C by incremental dosing of CO_2 using the ASAP 2020 analyzer. A dosing rate of 0.1 μmol with an equilibration time of 1.5 h was preset in the software of the gas analyzer. The amount of CO_2 adsorbed was determined from the pressure drop using Micromeritics software. Each dose generates a distinct calorimetric peak due to the heat effects associated with adsorption which was simultaneously recorded

dx.doi.org/10.1021/jp508678k | J. Phys. Chem. C 2014, 118, 29836−29844

Table 1. Mg/Al Ratios and Lattice Parameters of [Mg−Al−CO_3] LDH

layered double hydroxide system	sample code	[Mg]/[Al]	*a* parameter (Å)	*c* parameter (Å)
$[Mg_{0.745}Al_{0.255}(OH)_2][CO_3]_{0.127}\cdot 0.6H_2O$[a]	MA_31 (Riechle method)[b]	2.9	3.055	23.16
$[Mg_{0.66}Al_{0.33}(OH)_2][CO_3]_{0.166}\cdot 0.85H_2O$	MA_21 (Riechle method)	2	3.036	22.62
$[Mg_{0.66}Al_{0.33}(OH)_2][CO_3]_{0.166}\cdot 0.5H_2O$	MA_UH (urea hydrolysis)	2	3.036	22.44

[a]Carbonate content is given based on the estimated Al content in the sample. [b]Method of synthesis.

Table 2. Summary of Calorimetric Data of CO_2 Adsorption on [Mg−Al−CO_3] LDH and MMO

sample	specific surface area (m^2/g)	differential enthalpy for first dose (kJ/mol)	surface coverage (CO_2/nm^2)[a]	integral enthalpy (kJ/mol)[a]	amount of CO_2 adsorbed (mmol/g)[a]
MA_21 LDH	71	−91.46	5.4	−65.1	0.65
MA_21 MMO	182	−119.8	2.4	−58.8	0.74
MA_31 LDH	68	−92.04	5.4	−57.7	0.62
MA_31 MMO	143	−89.2	4.0	−43.9	0.97
MA_UH LDH	10	−81.4	1.5	−54.8	0.026
MA_UH MMO	211	−96.5	1.4	−50.3	0.39

[a]Calculated for coverage when differential adsorption enthalpy value reaches −17 kJ/mol, see text.

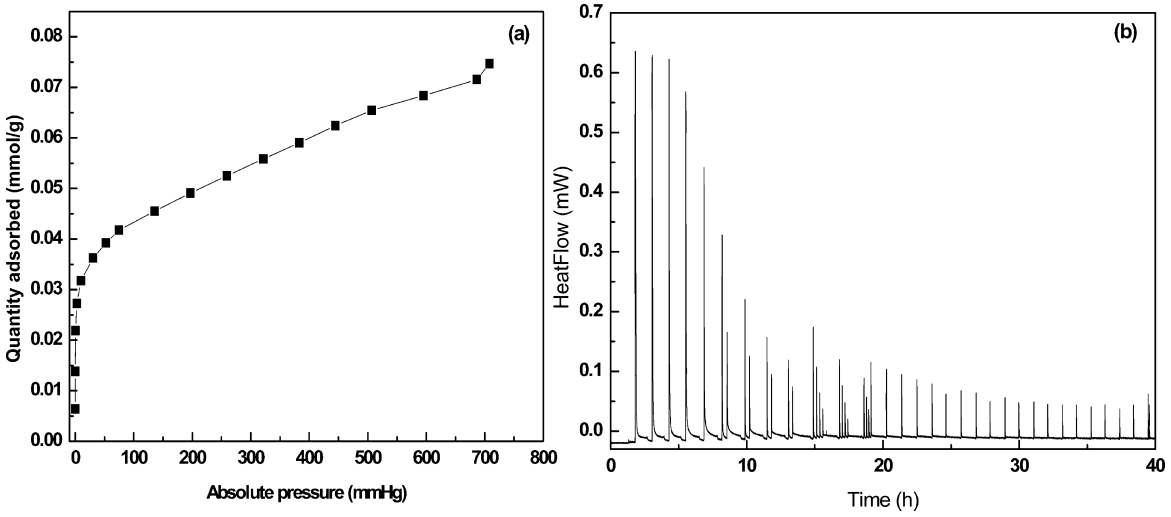

Figure 3. (a) Typical CO_2 adsorption isotherm of [Mg−Al−CO_3] layered double hydroxide and (b) its corresponding calorimetric trace.

using the microcalorimeter. The enthalpy of adsorption for each dose was calculated by integrating the area under the calorimetric peak. Heat effects obtained by integrating the calorimetric signal is divided by the amount of CO_2 dosed to obtain the differential enthalpy of adsorption.

RESULTS AND DISCUSSION

Figure 2 shows the PXRD patterns of all the three as synthesized LDH and the corresponding MMO after heat treatment at 400 °C. As-synthesized samples exhibit characteristic peaks corresponding to layered double hydroxide phase.

The basal reflections (00*l*) of all samples are sharp, indicating good registry of layers along *c* direction. Doublets, (110) and (113), above 60°2θ are sharp indicating none of the samples have turbostratic disorder. However, MA_21 and MA_31 exhibit broad peaks in the mid-2θ region indicative of stacking disorder. This lack of long-range stacking order is the reason why we refer to them as less crystalline. Conversely the presence of this long-range stacking order in MA_UH is the reason why we term MA_UH to be highly crystalline. All three LDH exhibit reflections corresponding to a three layer rhombohedral ($3R_1$) polytype. Their lattice parameters are listed in Table 1. Degassing layered double hydroxide samples at 400 °C leads to dehydroxylation, forming amorphous MMO (Figure 2b). ATR-FTIR spectra of all the samples are shown in Figure 2c. Pristine layered double hydroxide samples show a characteristic peak at 1360 cm^{-1} (ν_3) corresponding to intercalated carbonate ion. Free carbonate ion exhibits an antisymmetric stretching vibration, ν_3, at 1400 cm^{-1} and upon intercalation it shifts toward lower wavenumber and is observed at 1360 cm^{-1} in LDH.[34] The absence of a peak at 1360 cm^{-1} in heat treated LDH confirms decarboxylation and thus formation of MMO. TGA of all three LDH shows two step mass losses (Supporting Information Figure S1). In all the cases mass loss below 250 °C is attributed to water loss. The mass loss below 100 °C is considered to be due to adsorbed water and that at 100−250 °C is attributed to intercalated water. The water content present in different LDH is listed in Table 1. Any mass loss observed between 250 and 450 °C is attributed to combined CO_2 and H_2O loss. A previous study of layered double hydroxide decomposition by TG coupled with MS and IR observed dehydroxylation and decarbonation occur simultaneously at 250−450 °C.[35] Specific surface areas of all the LDH and their corresponding MMO are listed in Table 2. MMO derived from all three LDH exhibit high specific surface area. However, MA_UH layered double hydroxide has lower

dx.doi.org/10.1021/jp508678k | J. Phys. Chem. C 2014, 118, 29836−29844

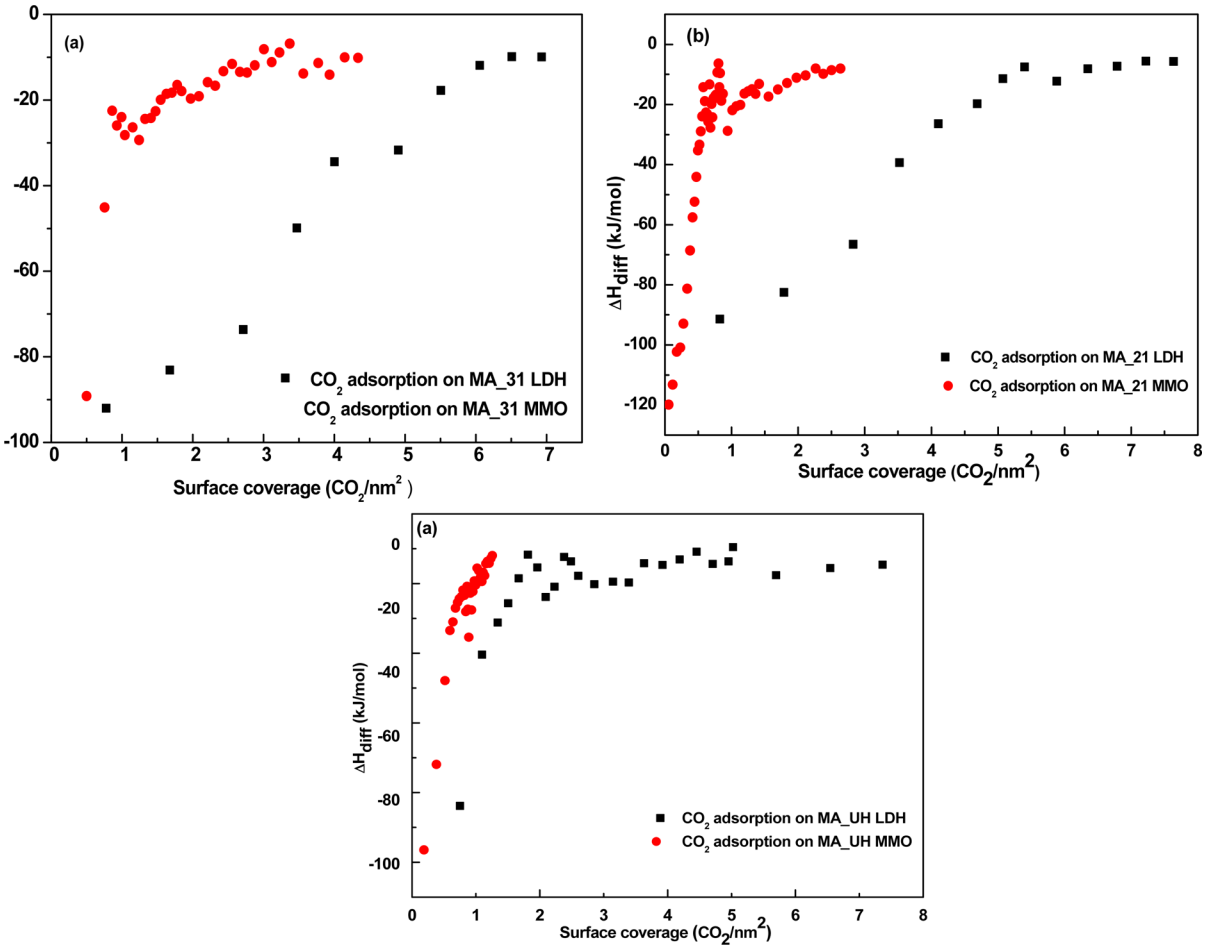

Figure 4. CO_2 adsorption enthalpy for LDH and their corresponding MMO (a) MA_31, (b) MA_21, and (c) MA_UH.

specific surface area than MA_31 and MA_21 LDH. The sample synthesized by urea hydrolysis is highly ordered and has a defined interlayer structure unlike the other two LDH which are replete with stacking disorder. One likely hypothesis for the observed lower surface area of MA_UH layered double hydroxide is the better stacking and the ordered interlayer which minimizes the penetration of gas molecules. However, once it is decomposed/calcined the formed mixed metal oxide is amorphous and possesses larger surface area.

CO_2 Adsorption on LDH. A typical CO_2 adsorption isotherm and a calorimetric trace are shown in Figure 3. The initial uptake in the isotherm corresponds to chemisorbed CO_2 and has the most negative differential enthalpy. With each dose the differential enthalpy becomes less exothermic with increasing coverage. Measurements were made until the value of enthalpy of adsorption of CO_2 reached the heat of condensation of CO_2, −17 kJ mol^{-1}, after which CO_2 is considered to be physisorbed.[36] Calorimetric data for all samples are summarized in Table 2. The differential enthalpies of CO_2 adsorption as a function of surface coverage for MA_21 and MA_31 LDH and their corresponding MMO are shown in Figure 4.

At near zero coverage the enthalpy of CO_2 adsorption for the first dose on pristine LDH is −92 kJ/mol, −91 kJ/mol, and −81 kJ/mol for MA_31, MA_21, and MA_UH, respectively. This implies strong chemisorption of CO_2 during initial uptake, involving an interaction similar to an acid−base reaction.

With increase in surface coverage in each case the adsorption becomes less exothermic and there is a continuous decrease in the magnitude of the differential adsorption enthalpy, indicating the presence of energetically different active sites. In the LDH, the interlayer also acts as accessible surface. It is further known to be highly basic ($[OH]^-$ = 11.8 M)[37] and thus also acts as sites for active CO_2 adsorption. For both MA_31 and MA_21 LDH, there is a continuous decrease in the magnitude of negative differential enthalpy before reaching the value of −17 kJ/mol. At this point, surface coverage of 5.4 CO_2/nm^2 and 5.5 CO_2/nm^2 with an integral enthalpy of −57 kJ/mol and −65 kJ/mol is observed for MA_31 and MA_21 LDH, respectively. For MA_UH LDH however there is an approximately exponential decrease in the magnitude of the negative differential enthalpy value and it reaches −17 kJ/mol within 4−5 doses. A surface coverage of 1.5 CO_2/nm^2 with an integral enthalpy of −54 kJ/mol is observed at this point. MA_31 and MA_21 LDH are replete of extensive stacking disorder. They have comparable surface areas (see Table 2) and show similar behavior during CO_2 adsorption. MA_UH layered double hydroxide is highly crystalline with a well-defined interlayer and possesses very low surface area. It shows different and poor CO_2 adsorption as opposed to the other two LDH. However, its initial CO_2 adsorption enthalpy is similar to that for the other two LDH, probably because the initial uptake is on surface Mg−O sites.

In all cases at higher coverage, we observe a split in the calorimetric peaks (Figure 2b). This can be attributed to an exothermic secondary process occurring soon after the initial

dx.doi.org/10.1021/jp508678k | J. Phys. Chem. C 2014, 118, 29836−29844

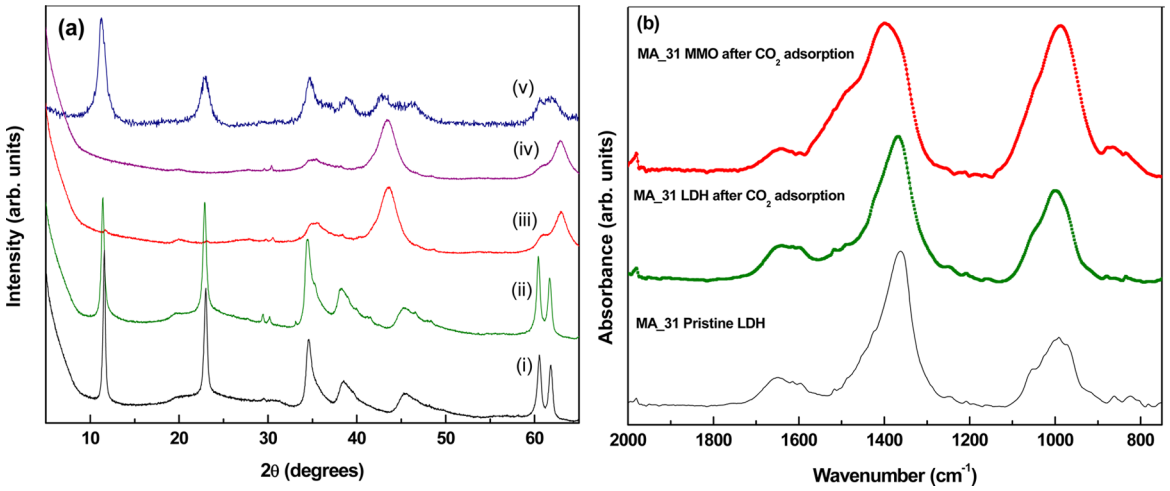

Figure 5. (a) XRD patterns of MA_31LDH (i) after degas at 100 °C, (ii) after degassing followed by CO_2 adsorption, (iii) after degas at 400 °C (MMO), (iv) after CO_2 adsorption by MA_31 MMO, and (v) CO_2 adsorbed MA_31 MMO exposed to ambient. (b) ATR spectra of MA_31 LDH and MA_31 MMO after CO_2 adsorption.

adsorption. This process could be redistribution of adsorbed CO_2 on energetically different sites and/or interaction of CO_2 with water molecules and hydroxyl groups of the LDH. However, we have no direct evidence for its microscopic origin.

The samples were characterized by PXRD and ATR-FTIR after the adsorption experiments to detect any phase changes associated with CO_2 adsorption. The PXRD pattern of MA_31 LDH after CO_2 uptake is shown in Figure 5. It does not exhibit any appreciable changes indicating that there is no formation of any auxiliary phases like $MgCO_3$ or that any such phase formed at the surface is amorphous. It could also be possible that there is formation of crystalline $MgCO_3$ whose domain size is smaller than the XRD detection limit that could have led to broadening of the corresponding reflections. However, we observe broadening of the basal reflection of MA_31 LDH after CO_2 adsorption with a shift from 7.61 to7.75 Å. This shift can be attributed to insertion of CO_2 into the interlayer and the broadening could be due to interstratification arising due to CO_2 insertion. PXRD patterns of MA_21 and MA_UH LDH do not show any appreciable changes (S2) after CO_2 adsorption as well, except for the shift in the basal reflections. Although there are several reports on different aspects of CO_2 uptake properties of Mg−Al LDH and their MMO, this work primarily focuses on energetics of CO_2 sorption by these materials which gives the information on strength of basic sites available and is complemented with ATR-FTIR studies. The ATR-FTIR spectrum of MA_31 LDH after CO_2 adsorption is shown in Figure 5b. The overlapping bands upon decomposition shows peaks at 1060, 1295, 1360, 1410, 1490, 1540, 1595 and 1650 cm^{-1} (S3) indicating the presence of more than one kind of carbonate. Free carbonate ion having D_{3h} symmetry is known to exhibit IR peaks at 1065 cm^{-1} (ν_1, symmetric stretching), 880 cm^{-1} (ν_2, out of plane bending mode) and 1390 cm^{-1} (ν_3, antisymmetric stretching). The peak observed at 1060 cm^{-1} in CO_2 adsorbed MA_31 LDH can be attributed to the C−O stretching mode (ν_1). The O−C−O antisymmetric stretching (ν_3), which is degenerate, appears at 1410 cm^{-1} with several additional peaks at 1305, 1540, 1490, 1595, and 1650 cm^{-1}. CO_2 as an adsorbate has been used as a probe in the literature to examine the surface basicity.[38,39] The value of $\Delta\nu_3$, the deviation from 1400 cm^{-1}, can be used to determine the mode of binding of CO_2 and thus to evaluate the nature of basic sites. A lower $\Delta\nu_3$ value (50−150 cm^{-1}) indicates monodentate carbonate bonding, and a higher $\Delta\nu_3$ value (200−400 cm^{-1}) indicates bidentate (bridging/chelating) bonding.[39] The observed value of $\Delta\nu_3$ (105−360 cm^{-1}) in the present case thus indicates the presence of both monodentate and bidentate carbonate in CO_2 adsorbed MA_31 LDH. Similarly the ATR-FTIR spectrum of MA_21 LDH after CO_2 uptake shows additional features (S4) with peaks at 780 (ν_2), 960 (ν_1), 1300, 1360, 1400, 1540, and 1610 cm^{-1} (ν_3). The observed value of $\Delta\nu_3$ (100−300 cm^{-1}) in this case suggests two kinds of carbonate bound in monodentate and bidentate fashion. MA_UH layered double hydroxide after CO_2 uptake shows bands at 1300, 1360, 1408, 1477, 1540, and 1580 cm^{-1} in the ATR-FTIR spectrum (S5). These can be attributed to the presence of monodentate and bridging bidentate carbonate species as well.

In summary both MA_31 and MA_21 LDH show similar initial adsorption characteristics. Marginally higher CO_2 uptake and higher integral adsorption enthalpy in the case of MA_21 layered double hydroxide could be associated with its comparatively higher water content as the water content is known to promote CO_2 adsorption in LDH.[40] MA_UH shows poor CO_2 uptake characteristics owing to its lower surface area.

CO_2 Adsorption on MMO. MMO derived from thermal decomposition of LDH at 400 °C exhibit different CO_2 adsorption behavior than their pristine LDH counterparts. The initial differential adsorption enthalpy values at near zero coverage are −94, −119, and −97 kJ/mol for MA_31, MA_21, and MA_UH MMO, respectively. In all three cases the magnitude of exothermic differential enthalpy drops roughly exponentially with further doses before attaining a stable value of about −17 kJ/mol. While this does indicate that there are active sites which are energetically different, there is no interlayer in MMO as in LDH, and hence the nature of these sites is less clear. There are reports that during the calcination of LDH to MMO, there is formation of active Mg−O species, which are responsible for larger CO_2 uptake compared to that of pristine LDH.[26] The active Mg−O species can be formed by two different mechanisms. The first is the partial substitution of Mg^{2+} by Al^{3+} in the MgO periclase lattice, leading to positive charge, for which to compensate the adjacent O^{2-} ions become coordinatively unsaturated. For each Al^{3+} insertion in this case

dx.doi.org/10.1021/jp508678k | J. Phys. Chem. C 2014, 118, 29836−29844

two active Mg−O sites are thus formed. The second possible mechanism is partial diffusion of Al^{3+} from octahedral sites in LDH to tetrahedral sites in MMO in the interlayer during calcination. This leads to vacancies in the Al site forming three active Mg−O species around it. Either of these mechanisms thus leads to Mg−O sites of different energetics for CO_2 uptake on the MMO surface, perhaps explaining our observations. Such defect mechanisms also may explain our observation of more exothermic initial differential enthalpy of adsorption for MA_21 MMO (−119.8 kJ/mol) compared to MA_31 MMO (−89.2 kJ/mol), as the number of Mg−O active sites formed should be greater in the former due to its larger Al content. The observed integral enthalpy of adsorption for MA_21 (−58 kJ/mol), and MA_31 MMO (−43 kJ/mol) also could be explained to the same reason. However, the amount of CO_2 adsorbed is larger in MA_31 MMO than in MA_21 MMO due to higher Mg content, which is consistent with the reports in the literature that higher Mg content promotes CO_2 adsorption.[23] On the other hand, despite exhibiting a higher surface area (211 m^2/g) the MA_UH mixed metal oxide does not show good adsorption capacity. Surface coverages of 4.0, 2.4, and 1.4 CO_2/nm^2 with integral enthalpies of −43, −58, and −50 kJ/mol are observed for MA_31, MA_21, and MA_UH MMO, respectively, when the differential enthalpy approaches −17 kJ/mol, the enthalpy of condensation of CO_2.

PXRD patterns of all the MMO after CO_2 adsorption show no phase change or new phase formation, ruling out the formation of $MgCO_3$ on the surface of MMO or indicating that any phase formed is amorphous. Figure 5a, traces iii and iv show PXRD patterns of MA_31 MMO before and after CO_2 uptake. There is no reconstruction to the layered double hydroxide phase after CO_2 adsorption (memory effect) due to lack of moisture. However, once the sample is exposed to ambient (Figure 5a,v) it picks up water and reconstruction to the layered double hydroxide phase is observed as expected.[15] Similarly both MA_21 and MA_UH MMO show no change in the PXRD pattern after CO_2 adsorption (Supporting Information, Figure S2). The ATR-FTIR spectrum of CO_2 adsorbed MA_31 MMO (Figure 5b) shows a shift in the C−O stretching vibration from 1360 to 1380 cm^{-1} as compared to LDH. Additional features appear (Supporting Information, Figure S3b) at 987 (ν_2), 1044 (ν_1), and 1438, 1513, and 1638 cm^{-1} (ν_3). On the basis of the the observed IR bands ($\Delta\nu_3$ = 60−260 cm^{-1}), as explained earlier, the sample has two kinds of carbonate bound to the surface, monodentate [on stronger basic sites, possibly Mg−O···$CO_{2(ads)}$] and chelating bidentate, [on weaker basic sites, possibly Mg/Al−O···(O−C−O)$_{ads}$...O−Mg/Al]. Thus, the spectra also support the presence of two different sites for CO_2 on the mixed metal oxide surface. Similar results were observed for MA_21 MMO (Supporting Information, Figure S4) with peaks at 1305, 1367, 1415, 1560, and 1650 cm^{-1}, indicating comparable sites available for CO_2 adsorption as in MA_31 MMO. The ATR-FTIR spectrum of MA_UH MMO (Supporting Information, Figure S5) exhibits bands at 1390, 14160, 1525, and 1600 cm^{-1} which can be attributed to monodentate carbonate on the surface of the MMO. The presence of only one kind of carbonate species in this case, unlike the other two, could be related to a possibly ordered arrangement of active Mg−O sites in the mixed metal oxide of the MA_UH LDH, having a composition 2:1, which is known to be cation ordered.[41]

In both LDH and MMO we observe heterogeneous active sites available for CO_2 adsorption. While in LDH the different sites arise from sites available on the layered double hydroxide surface and the interlayer, on MMO they arise from different Mg−O sites available on the surface, formed during decomposition. It is interesting that the enthalpy at low coverage is similar for LDH and MMO but the intermediate coverage behavior is different. This difference could possibly be related to the presence of an interlayer in LDH and its absence in MMO. Initial adsorption in both the cases happens on the surface, while with increasing coverage in LDH, adsorption proceeds on the interlayer and is associated with more exothermic adsorption enthalpy.

The nature of basic sites available and their distribution depends on several factors including composition, water content, crystallinity, and nature of cations in the layer. Higher Mg content is known to promote CO_2 uptake capacity which is observed in our study as well. A recent report of CO_2 adsorption on partially Ga substituted Mg−Al LDH shows an outstanding sorption capacity of 2.0 mmol cm^{-3}.[42] The presence of moisture, which is important for several CO_2 uptake applications, does not affect the capacity much.[43] In some cases moisture/water vapor is known to promote CO_2 uptake capacity among LDH and MMO.[40] In the present case we see a marginal increase in CO_2 adsorption capacity of MA_21 LDH compared to MA_31 LDH, which we have attributed to larger water content in the latter. In the MMO, where all the experiments were carried under dry conditions, we do not see reconstruction to the layered double hydroxide phase after CO_2 uptake.

Adsorbent regeneration is another important aspect for applications. Both LDH and MMO are generally heated under vacuum to regenerate them for further CO_2 adsorption cycles. Miguel and co-workers[42] have done systematic studies on sorption−desorption of CO_2 for several cycles. They conclude that 25% of sorption capacity is lost irreversibly during the second cycle. We observe similar results. For instance, MA_31 layered double hydroxide shows a sorption capacity of 0.62 mmol/g with an integral enthalpy of −58 kJ/mol in the first cycle. After regenerating the adsorbent in the second cycle, it exhibits a sorption capacity of 0.48 mmol/g with an integral enthalpy of −49 kJ/mol. However, in both the cycles the differential enthalpy for first dose remains the same, indicating that the sites to which CO_2 is strongly bound are available after regeneration of the sorbent. This also indicates that the sites where the initial adsorption occurs show reversible behavior, while sites where slow adsorption (including those with the split calorimetric peaks) occurs show irreversible binding. Similar observations were made by Ritter and co-workers.[44] Using in situ FTIR they showed that peaks corresponding to a monodentate bond (on stronger sites) carbonate disappeared during sorbent regeneration by heating, whereas polydentate carbonate (more weakly bound) remained intact.

It would be interesting to study energetics of Ca−Al LDH as they are reported to have the highest CO_2 uptake among LDH.[45] Furthermore, the 7-fold coordination of Ca^{2+}, its complex interlayer, and larger water content make these phases interesting candidates for such analysis.

CONCLUSIONS

This work sheds light upon some important aspects of CO_2 uptake properties of LDH and MMO. While the amount of CO_2 adsorbed varies with composition, the initial differential enthalpy is similar, indicating that the available sites are similar for initial strong binding and uptake. The integral enthalpy with

dx.doi.org/10.1021/jp508678k | J. Phys. Chem. C 2014, 118, 29836−29844

increasing coverage varies substantially among different LDH and MMO, reflecting the nature and number of basic sites available for adsorption. Examining carbonate stretching frequencies after CO_2 adsorption gives insights on the nature of binding and strength of basic sites which supplements the data obtained by adsorption calorimetry.

■ ASSOCIATED CONTENT

Supporting Information

TG-DTG curves of all the three LDH; PXRD patterns of MA_21 and MA_UH LDH and MMO after CO_2 adsorption; ATR-FTIR spectra of all the three LDH and MMO after CO_2 adsorption. This material is available free of charge via the Internet at http://pubs.acs.org.

■ AUTHOR INFORMATION

Corresponding Author

*E-mail: anavrotsky@ucdavis.edu.

Notes

The authors declare no competing financial interest.

■ ACKNOWLEDGMENTS

We thank Donald Land for providing the facility for ATR-FTIR measurements. We thank Sergey Ushakov for his help with adsorption experiments. The funding for this work is provided by the U.S. Department of Energy under Grant No. DE-FG02-97ER14749.

■ REFERENCES

(1) D'Alessandro, D. M.; Smit, B.; Long, J. R. Carbon Dioxide Capture: Prospects for New Materials. *Angew. Chem., Int. Ed. Engl.* **2010**, *49*, 6058−6082.

(2) Choi, S.; Drese, J. H.; Jones, C. W. Adsorbent Materials for Carbon Dioxide Capture from Large Anthropogenic Point Sources. *ChemSusChem* **2009**, *2*, 796−854.

(3) Reddy, M. K. R.; Xu, Z. P.; Lu, G. Q. M.; Costa, J. C. D. Layered Double Hydroxides for CO_2 Capture: Structure Evolution and Regeneration. *Ind. Eng. Chem. Res.* **2006**, 7504−7509.

(4) Wang, Q.; Wu, Z.; Tay, H. H.; Chen, L.; Liu, Y.; Chang, J.; Zhong, Z.; Luo, J.; Borgna, A. High Temperature Adsorption of CO_2 on Mg−Al Hydrotalcite: Effect of the Charge Compensating Anions and the Synthesis pH. *Catal. Today* **2011**, *164*, 198−203.

(5) Garcia-Gallastegui, A.; Iruretagoyena, D.; Mokhtar, M.; Asiri, A. M.; Basahel, S. N.; Al-Thabaiti, S. A.; Alyoubi, A. O.; Chadwick, D.; Shaffer, M. S. P. Layered Double Hydroxides Supported on Multiwalled Carbon Nanotubes: Preparation and CO_2 Adsorption Characteristics. *J. Mater. Chem.* **2012**, *22*, 13932−13940.

(6) Li, B.; He, J.; Evans, D. G.; Duan, X. Enteric-Coated Layered Double Hydroxides as a Controlled Release Drug Delivery System. *Int. J. Pharm.* **2004**, *287*, 89−95.

(7) Gao, Y.; Wang, Q.; Wang, J.; Huang, L.; Yan, X.; Zhang, X.; He, Q.; Xing, Z.; Guo, Z. Synthesis of Highly Efficient Flame Retardant High-Density Polyethylene Nanocomposites with Organo-Layered Double Hydroxides as Nano Filler Using Solvent Mixing Method. *ACS Appl. Mater. Interfaces* **2014**, *6*, 5094−5104.

(8) Wang, S.; Liu, C.; Wang, M.; Chuang, Y.; Chiang, P. Arsenate Adsorption by Mg/Al−NO_3 Layered Double Hydroxides with Varying the Mg/Al Ratio. *Appl. Clay Sci.* **2009**, *43*, 79−85.

(9) Tanabe, K.; Ho, W. F. Industrial Application of Solid Acid−Base Catalysts. *Appl. Catal., A* **1999**, *181*, 399−434.

(10) Cavani, F.; Trifiro, F.; Vaccari, A. Hydrotalcite-Type Anionic Clays: Preparation, Properties and Applications. *Catal. Today* **1991**, *11*, 173−301.

(11) Evans, D. G.; Slade. R. C. T. Structural Aspects of Layered Double Hydroxides. In *Layered Double Hydroxides*; Duan, X., Evans, D. G, Eds.; Springer: New York, 2005.

(12) Miyata, S. Anion-Exchange Properties of Hydrotalcite-like Compounds. *Clays Clay Miner.* **1983**, *31*, 301−311.

(13) Zhao, X.; Zhang, F.; Xu, S.; Evans, D. G.; Duan, X. From Layered Double Hydroxides to ZnO-Based Mixed Metal Oxides by Thermal Decomposition: Transformation Mechanism and UV-Blocking Properties of the Product. *Chem. Mater.* **2010**, *22*, 3933−3942.

(14) Cosimo, J. I. D.; Diez, V. K.; Xu, M.; Iglesia, E.; Apesteguia, C. R. Structure and Surface and Catalytic Properties of Mg−Al Basic Oxides. *J. Catal.* **1998**, *178*, 499−510.

(15) Chibwe, K.; Jones, W. The Synthesis of Polyoxometalate Pillared Layered Double Hydroxides via Calcined Precursors. *Chem. Mater.* **1989**, *1*, 489−490.

(16) Reddy, M. K. R.; Xu, Z. P.; Lu, G. Q. M.; Costa, J. C. D. Influence of Water on High-Temperature CO_2 Capture Using Layered Double Hydroxide Derivatives. *Ind. Eng. Chem. Res.* **2008**, 2630−2635.

(17) Pfeiffer, H.; Ávalos-rendón, T.; Lima, E.; Valente, J. S. Thermochemical and Cyclability Analyses of the CO_2 Absorption Process on a Ca/Al Layered Double Hydroxide. *J. Environ. Eng.* **2012**, *137*, 1058−1065.

(18) Sharma, U.; Tyagi, B.; Jasra, R. V. Synthesis and Characterization of Mg−Al−CO_3 Layered Double Hydroxide for CO_2 adsorption. *Ind. Eng. Chem. Res.* **2008**, *47*, 9588−9595.

(19) Chang, P.-H.; Lee, T.-J.; Chang, Y.-P.; Chen, S.-Y. CO_2 Sorbents with Scaffold-like Ca−Al Layered Double Hydroxides as Precursors for CO_2 Capture at High Temperatures. *ChemSusChem* **2013**, *6*, 1076−1083.

(20) Lee, J. M.; Min, Y. J.; Lee, K. B.; Jeon, S. G.; Na, J. G.; Ryu, H. J. Enhancement of CO_2 Sorption Uptake on Hydrotalcite by Impregnation with K_2CO_3. *Langmuir* **2010**, *26*, 18788−18797.

(21) Halabi, M. H.; de Croon, M. H. J. M.; van der Schaaf, J.; Cobden, P. D.; Schouten, J. C. High Capacity Potassium-Promoted Hydrotalcite for CO_2 Capture in H_2 Production. *Int. J. Hydrogen Energy* **2012**, *37*, 4516−4525.

(22) Halabi, M. H.; de Croon, M. H. J. M.; van der Schaaf, J.; Cobden, P. D.; Schouten, J. C. A Novel Catalyst−Sorbent System for an Efficient H_2 Production with in-Situ CO_2 Capture. *Int. J. Hydrogen Energy* **2012**, *37*, 4987−4996.

(23) Aschenbrenner, O.; McGuire, P.; Alsamaq, S.; Wang, J.; Supasitmongkol, S.; Al-Duri, B.; Styring, P.; Wood, J. Adsorption of Carbon Dioxide on Hydrotalcite-like Compounds of Different Compositions. *Chem. Eng. Res. Des.* **2011**, *89*, 1711−1721.

(24) Wang, Q.; Tay, H. H.; Guo, Z.; Chen, L.; Liu, Y.; Chang, J.; Zhong, Z.; Luo, J.; Borgna, A. Morphology and Composition Controllable Synthesis of Mg−Al−CO_3 Hydrotalcites by Tuning the Synthesis pH and the CO_2 Capture Capacity. *Appl. Clay Sci.* **2012**, *55*, 18−26.

(25) Hutson, N. D.; Attwood, B. C. High Temperature Adsorption of CO_2 on Various Hydrotalcite-like Compounds. *Adsorption* **2008**, *14*, 781−789.

(26) Gao, Y.; Zhang, Z.; Wu, J.; Yi, X.; Zheng, A.; Umar, A.; O'Hare, D.; Wang, Q. Comprehensive Investigation of CO_2 Adsorption on Mg−Al−CO_3 LDH-Derived Mixed Metal Oxides. *J. Mater. Chem. A* **2013**, *1*, 12782.

(27) Maroño, M.; Torreiro, Y.; Gutierrez, L. Influence of Steam Partial Pressures in the CO_2 Capture Capacity of K-Doped Hydrotalcite-Based Sorbents for Their Application to SEWGS Processes. *Int. J. Greenhouse Gas Control* **2013**, *14*, 183−192.

(28) Wu, Y.-J.; Li, P.; Yu, J.-G.; Cunha, a. F.; Rodrigues, a. E. K-Promoted Hydrotalcites for CO_2 Capture in Sorption Enhanced Reactions. *Chem. Eng. Technol.* **2013**, *36*, 567−574.

(29) Ishihara, S.; Sahoo, P.; Deguchi, K.; Ohki, S.; Tansho, M.; Shimizu, T.; Labuta, J.; Hill, J. P.; Ariga, K.; Watanabe, K.; et al. Dynamic Breathing of CO_2 by Hydrotalcite. *J. Am. Chem. Soc.* **2013**, *135*, 18040−18043.

(30) Wu, D.; Gassensmith, J. J.; Gouvêa, D.; Ushakov, S.; Stoddart, J. F.; Navrotsky, A. Direct Calorimetric Measurement of Enthalpy of Adsorption of Carbon Dioxide on CD-MOF-2, a Green Metal−Organic Framework. *J. Am. Chem. Soc.* **2013**, *135*, 6790−6793.

(31) Reichle, W. T. Synthesis of Anionic Clay Minerals (Mixed Metal Hydroxides, Hydrotalcite). *Solid State Ionics* **1986**, *22*, 135−141.
(32) Costantino, U.; Marmottini, F.; Nocchetti, M.; Vivani, R. New Synthetic Routes the Hydrotalcite-Like Compounds—Characterization and Properties of the Obtained Materials. *Eur. J. Inorg. Chem.* **1998**, *10*, 1439−1446.
(33) Gouvêa, D.; Ushakov, S. V.; Navrotsky, A. Energetics of CO_2 and H_2O Adsorption on ZnO. *Langmuir* **2014**, *30*, 9091−9097.
(34) Kloprogge, T.; Frost, R. L. Infrared and Raman Spectroscopic Studies of LDHs. In *Layered Double Hydroxides: Present and Future*; Rives, V., Ed.; Nova Science Publishers: Hauppauge, NY, 2001.
(35) Rives, V. Study of Layered Double Hydroxides By Thermal Methods. In *Layered Double Hydroxides: Present and Future*; Nova Science Publishers: Hauppauge, NY, 2001.
(36) Arrigo, R.; Havecker, M.; Wrabetz, S.; Blume, R.; Lerch, M.; McGregor, J.; Parrott, E. P. J.; Zeitler, J. A.; Gladden, L. F.; Knop-Gericke, A.; Schlogl, R.; Su, D. S. Tuning the Acid/Base Properties of Nanocarbons by Functionalization via Amination. *J. Am. Chem. Soc.* **2010**, *132*, 9616−9630.
(37) Prasad, B. E.; Dinamani, M.; Vishnu Kamath, P.; Mehta, S. H. Hexacyanoferrate (III) as an Electroactive Probe for the Investigation of the Interlayer Basicity of the Layered Double Hydroxide (LDH) of Mg with Al. *J. Colloids Interface Sci.* **2010**, *348*, 216−218.
(38) Lavalley, J. C. Infrared Spectrometric Studies of the Surface Basicity of Metal Oxides and Zeolites Using Adsorbed Probe Molecules. *Catal. Today* **1996**, *27*, 377−401.
(39) Su, C.; Suarez, D. L. In Situ Infrared Speciation of Adsorbed Carbonate on Aluminum and Iron Oxides. *Clays Clay Miner.* **1997**, *45*, 814−825.
(40) Reddy, M. K. R.; Xu, Z. P.; Lu, G. Q. M.; Costa, J. C. D. Influence of Water on High Temperature CO_2 Capture Using Layered Double Hydroxide Derivatives. *Ind. Eng. Chem. Res.* **2008**, *47*, 2630−2635.
(41) Sideris, P. J.; Nielsen, U. G.; Grey, C. P. Mg/Al Ordering in Layered Double Hydroxides Revealed by Multinuclear NMR Spectroscopy. *Science* **2008**, *321*, 113−117.
(42) Miguel, C. V.; Trujillano, R.; Rives, V.; Vicente, M. A.; Ferreira, A. F. P.; Rogrigues, A. E.; Mendes, A.; Madeira, L. M. High Temperature CO_2 Sorption with Gallium-Substituted and Promoted Hydrotalcites. *Sep. Purif. Technol.* **2014**, *127*, 202−211.
(43) Hufton, J. R.; Mayorga, S.; Sircar, S. Sorption-Enhanced Reaction Process for Hydrogen Production. *AIChE J.* **1999**, *45*, 248−256.
(44) Du, H.; Williams, C. T.; Ebner, A. D.; Ritter, J. A. In situ FTIR Spectroscopic Analysis of Carbonate Transformations During Adsorption and Desorption of CO_2 in K-Promoted HTLc. *Chem. Mater.* **2010**, *22*, 3519−3526.
(45) Chang, P. H.; Chang, Y. P.; Chen, S. Y.; Yu, C. T.; Chyou, Y. P. Ca-Rich Ca−Al-Oxide, High-Temperature-Stable Sorbents Prepared from Hydrotalcite Precursors: Synthesis, Characterization, and CO_2 Capture Capacity. *ChemSusChem* **2011**, *4*, 1844−1851.